RSC Advances

PAPER

View Article Online
View Journal | View Issue

Cite this: *RSC Adv.*, 2025, **15**, 27933

Biomass-derived 5-(tolylmethyl)furfural as a promising diesel additive: preparation, process scale-up, and engine studies

Abhishek Kumar Yadav,[a] Sandeep Kumar Yadav,[a] G. N. Kumar,[b] Vasudeva Madav[b] and Saikat Dutta *[a]

Received 6th June 2025
Accepted 30th July 2025

DOI: 10.1039/d5ra04020e

rsc.li/rsc-advances

Furanic fuel oxygenates, renewably produced from biomass, have received significant interest in lessening dependence on petroleum-derived liquid fuels and reducing emissions. 5-(Tolylmethyl)furfural (TMF) was prepared by the Friedel–Crafts reaction between cellulose-derived 5-(acetoxymethyl)furfural (AcMF) and petroleum-derived toluene. The process was optimized on various parameters, such as reaction temperature, molar ratio of reagents, catalyst loading, and duration. Anhydrous $ZnCl_2$ was the best catalyst for the reaction, affording a 67% isolated yield of TMF under optimized conditions (120 °C, 4 h). TMF was prepared on a 30 g scale and blended (1–5 vol%) with diesel. The physicochemical properties of the TMF-diesel blended fuel mixtures were studied, and then they were employed as fuel for a direct injection single-cylinder diesel engine. The results show good fuel properties and reduced emissions compared to unblended diesel fuel.

Introduction

Nearly 80% of a barrel of crude oil is transformed into liquid fuels (*e.g.*, gasoline, diesel, and jet fuel) for transportation.[1] Even with tremendous advances in emission-free technologies and the electrification of various sectors over the past decade, liquid hydrocarbon-based fuels will remain relevant for the transportation infrastructure.[2] However, there is a coordinated push to reduce the dependence on crude oil for liquid transportation fuels due to the ensuing social, economic, and environmental distress.[3] In this regard, cellulosic biomass has received significant interest as renewable carbon-based feedstock for synthesizing liquid transportation fuels.[4] The liquid biofuels can be used as a drop-in replacement for petrofuels or as a fuel oxygenate to be blended with petrofuels.[5] The oxygenated biofuel additives ensure complete combustion and reduce the emission of harmful compounds (*e.g.*, CO, particulates).[6] For example, carbohydrate-derived ethanol is compulsorily blended with gasoline in many countries to reduce dependency on petroleum and cleaner combustion.[7] The carbohydrate-derived furanic compounds have shown promise as advanced fuel oxygenates to be blended with petrofuels like diesel.[8] Carbohydrate-derived 5-(hydroxymethyl)furfural (HMF) is an established renewable platform chemical that can be transformed into a wide array of organic chemicals of commercial significance.[9] The production of HMF from abundant and inexpensive hexose sugars (*e.g.*, glucose), polymeric carbohydrates (*e.g.*, cellulose), and even untreated cellulosic biomasses is an elegant chemistry.[10] The acid-catalyzed process hydrolyses the polymeric carbohydrates into monomeric sugars, which then dehydrate at elevated temperatures into HMF. HMF retains all the biogenic carbon atoms of the parent sugar molecule, retains some reactive functionalities, and produces water as the sole innocuous byproduct.[11] Moreover, the transformation allows accessing aromatic compounds (*i.e.*, furanics) starting from aliphatic compounds. Even though HMF is not a biofuel by itself, many of its derivatives, where the furan ring remains intact, are promising biofuels and fuel oxygenates.[12,13] In many cases, HMF is partially reduced to form furanic biofuels under catalytic hydrogenation conditions.[12] HMF was reacted with alkylated benzenes (*e.g.*, toluene, xylenes) by Friedel–Crafts alkylation reaction using Zr-mont as the heterogeneous Lewis acid catalyst to make furanic biofuels.[13] Homogeneous acid catalysts, such as triflic acid, were also used for the Friedel–Crafts reaction with arenes.[14] Various mesoporous aluminosilicates were employed as heterogeneous Brønsted acid catalysts for the Friedel–Crafts alkylation of HMF with arenes.[15] In this regard, even though HMF has received immense attention as a furanic platform chemical, it is yet to be commercialized.[16] The challenge lies in the inherent hydrolytic, storage, and thermal instability of HMF. Moreover, the hydrophilicity of HMF complicated its isolation and purification at scale.[17] The yield of the Friedel–Crafts products was higher when starting with hydrophobic analogs of HMF. Moreover, the hydrophobic analogs of HMF require a Lewis acid catalyst for

[a]*Department of Chemistry National Institute of Technology Karnataka (NITK), Surathkal, Mangalore-575025, India. E-mail: sdutta@nitk.edu.in*

[b]*Mechanical Engineering Department, National Institute of Technology Karnataka (NITK), Surathkal, Mangalore-575025, India*

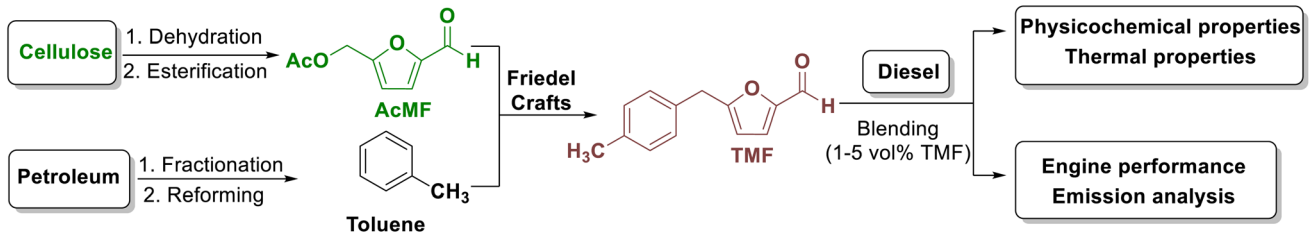

Scheme 1 Preparation of TMF as a hybrid biofuel and the use of TMF-diesel blends as engine fuel.

the Friedel–Crafts alkylation reaction with arenes, whereas HMF requires a Brønsted acid catalyst. Various hydrophobic analogs of HMF have received much interest as viable alternatives. These analogs can be formed directly from sugars and carbohydrates through the intermediary of HMF.[18]

Hybrid biofuels, typically a physical mixture of fuels from both biomass and petroleum, allow the optimal use of both feedstocks from economic and environmental perspectives.[19] Another strategy would be to make fuels of the desired molecular strategy, starting from molecules sourced from biomass and petroleum.[20] These fuels avoid overdependence on either petroleum or biomass and are more economically competent.[21] We reported various hybrid biofuels produced from carbohydrate-derived 5-(acetoxymethyl)furfural (AcMF) and petroleum-derived aromatic hydrocarbons. The Friedel–Crafts reaction was catalyzed by anhydrous zinc chloride, which provided good to excellent isolated yields of the targeted products under optimized conditions.[20] Specifically, 5-(tolylmethyl) furfural (TMF) can be produced by the Friedel–Crafts reaction between AcMF and toluene using a suitable Lewis acid catalyst. AcMF can be produced directly from hexose sugars and carbohydrates using a catalyst system containing excess acetic acid.[22,23] Alternatively, AcMF can be produced by a stepwise method, where another furanic intermediate from carbohydrates is transformed into AcMF.[24] AcMF possesses significantly better hydrolytic, storage, and thermal stability than HMF, and the former displays superior chemical reactivity to the latter in many cases. Toluene, a primary petrochemical, is produced primarily by reforming or alkylation reactions in the petrorefineries, and it has applications as a component in gasoline fuel, chemical feedstock, and solvent.[25] AcMF itself is a potential fuel oxygenate, but the ester functionality of its molecular structure may limit its use due to poor hydrolytic stability. The Friedel–Crafts reaction allows all the carbon atoms in the starting materials to be retained in the product molecule. The acetic acid byproduct can be conveniently recovered to prepare fresh AcMF. TMF is produced as a mixture of *ortho*- and *para*-isomers, which do not need to be separated for fuel applications.

Using fuel oxygenate improves engine performance and lowers emissions of harmful compounds. Recent studies have focused on incorporating fuel oxygenates derived from biomass and furanics into diesel fuels to enhance engine performance, improve combustion efficiency, and reduce emissions, while reducing the carbon footprint. Atmanli *et al.* used pentanol as a blend with diesel and demonstrated the effectiveness in enhancing ignition characteristics.[26] Ethanol/*n*-butanol with diesel as a diesel blend showed a better engine performance than diesel.[27] Alcohols, as oxygenated fuels widely used as additives, can be generated from various biomass resources *via* catalytic or enzymatic processes. Due to the lower energy density, lower cetane number, and poor miscibility with diesel, the alcohols can lead to phase separation and ignition delay. Diethyl ether was also used as an additive to a diesel-biodiesel fuel blend.[28] The high volatility and low boiling point of diethyl ether make it less ideal to use as an additive to diesel. In this regard, TMF exhibits superior fuel additive properties due to its better miscibility, chemical stability, and high energy density. This work reports the process optimization and scale-up studies of TMF starting from AcMF and toluene using $ZnCl_2$ as the Lewis acid catalyst. Zinc chloride supported on heterogeneous catalysts was also used and compared with $ZnCl_2$ alone. TMF was then blended (1–5 vol%) with petrodiesel, and the physicochemical and thermal characteristics of the blended fuels were examined. Finally, the blended fuels were examined in a stationary diesel engine for their combustion characteristics and emission analyses (Scheme 1).

Experimental section

Materials

Petroleum ether (60–80 °C, 99%), sodium chloride (98%), and ferric chloride (anhydrous, 98%) were purchased from Loba Chemie Pvt. Ltd. Chloroform (99%) was purchased from Finar. Toluene (99%), aluminium chloride (anhydrous, 98%), zinc chloride (anhydrous, 95%), nitromethane (99%), and silica gel (60–120 mesh) were procured from Spectrochem Pvt. Ltd. Lithium chloride (99%) and magnesium chloride (97%) were procured from spectrum. 5-(Acetoxymethyl)furfural (AcMF) was synthesized from fructose following a literature process.[23] Diesel was purchased from Indian Oil Corporation Limited (IOCL) outlet at Mangala Fuel and Services, Mukka, Karnataka.

Instrumentation

The synthesized TMF was characterized by Fourier transform infrared (FTIR) and nuclear magnetic resonance (NMR) spectroscopic techniques. The FTIR spectrum was acquired using the ATR method on a Bruker Alpha II FTIR spectrometer fitted with silicon carbide as an IR source. The sample was scanned 24 times with a scan rate of two scans per second and a spectral resolution of 4 cm^{-1}. The ^{1}H-NMR spectra were acquired in

a Bruker NanoBay® instrument operating at 400 MHz. The ^{13}C-NMR spectra were acquired in the same instrument at the calculated frequency of 100 MHz. The Bruker Topspin software (version 4.2.1) was used to process the raw NMR data.

Preparation of supported $ZnCl_2$ catalyst

Anhydrous $ZnCl_2$ (2 g) and silica gel (220–400 mesh, 8 g) was taken in a granite mortar and pestle. The mixture was ground for 30 min and then activated in a muffle furnace at 110 °C for 12 h before storing in an air-tight glass vial. The silica-supported catalyst was activated at 120 °C for 2 h in a hot-air oven prior to use.

Scale-up procedure for the synthesis of TMF

AcMF (30.00 g, 0.178 mol), toluene (65 mL, 0.712 mol), anhydrous $ZnCl_2$ (15 g, 50 wt%), and nitromethane (100 mL) were added in a 500 mL round bottom flask. The reaction mixture was heated at 120 °C in a preheated oil bath and magnetically stirred for 4 h. The reaction progress was monitored using thin-layer chromatography (TLC). After the completion of the reaction, the reaction mixture was washed with water and saturated bicarbonate solution and then extracted with ethyl acetate. The crude product was passed through a plug of silica gel in a sintered glass crucible to remove colored impurity. Finally, the excess toluene and nitromethane were evaporated under reduced pressure to get pure TMF as a reddish yellow oil (23.92 g, 67%).

Preparation of the Diesel–TMF blends

The prepared TMF was blended with diesel in 1–3 vol% and 5 vol%. TMF (50 mL) was measured in a measuring cylinder and introduced in a 2 L beaker. Diesel was added to make up for the volume of 1 L. A magnetic stirring bead was introduced, and the mixture was stirred magnetically at 400 rpm for 1 h to form the 5 vol% TMF-diesel blend (B5). Similarly, 10 mL, 20 mL, and 30 mL TMF were used to prepare 1 vol% TMF-diesel blend (B1), 2 vol% TMF-diesel (B2), and 3 vol% TMF-diesel (B3) blends, respectively.

Engine testing setup and instrumentation

TMF was blended in a 2 L beaker using a magnetic stirrer at 400 rpm, homogeneous mixing of the TMF with blend before testing the blended fuels in a single-cylinder diesel engine (make: Kirloskar, model; TV1). The engine setup includes an eddy current dynamometer for loading and a naturally aspirated, direct-injection water-cooled diesel engine system with a rated power of 3.5 kW at 1500 rpm. Table 1 shows the single-cylinder diesel engine's comprehensive parameters. In India, single-cylinder diesel engines are mainly used as prime movers for irrigation and energy production. This engine has also been widely employed in most academic institutions to research alternative fuels. A burette and stopwatch setup was used to measure the fuel consumption.

A Kistler's pressure sensor was installed at the top of the cylinder to obtain combustion data *via* the data-collecting system. A K-type (Cr–Al) thermocouple with a temperature indicator was used to record the lubrication oil and exhaust gas temperature. Using a data acquisition system, the combustion data was fed into combustion analysis software (Engine soft, Version 9.0). The emission of various gases was monitored by the INDUS 5 Gas Analyser (Model: PEA 205N). Fuel and air flow rates were measured manually for each load for each blend. The engine was allowed to run for 30 minutes to reach steady-state conditions before recording data. The exhaust gas analyzer specification used in the present research study is shown in the (SI, Table S1). The photographic images of the engine setup are shown in the SI (Fig. S1–S4).

Table 1 Specification of single-cylinder diesel engine

Specifications	Model: Kirloskar TV1
Ignition type	Compression engine
Diesel engine type	1 cylinder
No. of strokes	4
Compression ratio	17.5 : 01
Cylinder diameter	87.5 mm
Stroke length	100 mm
Governor	Centrifugal type
Intake system	Direct injection
Speed	1500 rpm
Orifice diameter	20 mm
Connecting rod length	234 mm
Displacement volume	661.45 cc
Dynamometer arm length	185 mm
Software	IC ENGINESOFT 9.0
Rated power	3.5 kW
Fuel pipe diameter	12.40 mm
Fuel ignition timing	23° before TDC
Fuel injection pressure	180 bar
Pulse per revolution	360°
Cooling	Water cooled
Lubricant	20W40

Results and discussion

Carbohydrate-derived furanic compounds have shown promise as biofuels and fuel oxygenates. Even though HMF is not a biofuel candidate due to its inherent low thermal and hydrolytic stability and strong hydrophilicity, many of its hydrophobic analogs are considered potential biofuels. For example, AcMF itself is a promising biofuel. However, the hydrolysis of AcMF during storage can produce acetic acid, which is corrosive to engine parts and fuel lines. Moreover, AcMF is fully bioderived, and its large-scale availability from biomass for fuel applications can cause logistical issues. Therefore, TMF was proposed as a hybrid biofuel, produced from both bioderived and petroleum-derived components, assuring the optimum use of both feedstocks. Anhydrous $ZnCl_2$ was found to be an effective Lewis acid catalyst for the Friedel–Crafts reaction between AcMF and toluene. TMF is produced as a mixture of both *ortho*- and *para*-isomer, where the latter is formed as the major product. The molar ratio of *para*- and *ortho*-isomer was nearly equimolar, based on the integration of peaks in the ^{1}H-NMR

spectrum. The following sections discuss the batch scale synthesis of TMF from AcMF and the preparation of 1–5 vol% TMF-diesel blends, analysis of the physicochemical properties of 1–5 vol% TMF-diesel blends, and the engine studies of TMF-diesel blends.

Preparation of TMF from AcMF

The TMF synthesis was undertaken by following the literature.[20] Initially, 0.5 g of AcMF was used under optimized conditions (50 wt% $ZnCl_2$, nitromethane 5 mL, 120 °C, 3 h), and it afforded a 76% isolated yield of TMF. After the stipulated reaction time, the reaction mixture was diluted with ethyl acetate and washed with water, followed by sodium bicarbonate solution to neutralize the acetic acid byproduct formed during the reaction. Moreover, the effect of various Lewis acid catalysts on the yield of TMF was also explored. When $AlCl_3$ and $FeCl_3$ were used as Lewis acid catalysts, the yield of TMF was decreased to 33% and 49%, respectively (entries 2 & 7, Table 2). When $MgCl_2$ was used as a catalyst, the yield improved marginally to 54% (entry 4, Table 2) compared to the stronger Lewis acid ($FeCl_3$ and $AlCl_3$) catalysts. When NaCl was used as the catalyst, no TMF was formed (entry 6, Table 2). When LiCl and $CaCl_2$ were also used as catalysts (entries 1 & 5, Table 2), the yield of TMF was decreased to 52% and 44%, respectively.

The Friedel–Crafts reaction was also carried out using heterogeneous catalysts by supporting $ZnCl_2$ on solid supports. Heterogeneous catalysts allow facile separation and catalyst recovery compared to their homogeneous counterpart. Initially, silica-supported $ZnCl_2$ was used under optimized conditions. The reaction didn't proceed at an appreciable rate and afforded a 62% yield of TMF (entry 8, Table 2). The catalyst was recovered by filtration. TMF was extracted using ethyl acetate and purified by column chromatography. The yield of TMF was substantially low when other solid supports were used. After optimizing the catalyst and other reaction parameters, the substrate loading was increased up to 10 g scale.

Preparation of TMF in a batch reactor

The preparation of TMF was undertaken by following the literature.[20] Zinc chloride (anhydrous) was used as an inexpensive Lewis acid catalysts for the Friedel–Crafts reaction between biomass-derived AcMF and petroleum-derived toluene using nitromethane as the solvent. The reaction was performed in a preheated oil bath (120 °C) and the reaction progress was monitored by TLC. Initially, the preparation of AcMF (precursor of TMF) was scaled up from 0.5 g to 10 g scale. The purification of TMF by column chromatography was effective but not suitable for a large scale due to the high cost and significant waste generation. Therefore, an alternative and scalable purification method of TMF was developed. The crude TMF was treated with activated carbon to remove color impurities, and excess toluene was distilled under reduced pressure. Finally, TMF was passed through a plug of silica gel to get pure TMF. The batch process was done on 30 g of AcMF under optimized conditions (120 °C, 4 h) and afforded a 67% yield of TMF. For the batch reaction, the reaction duration was increased from 3 h to 4 h compared to the 0.5 g scale synthesis of TMF.

Table 2 The effect of various catalysts on the yield of TMF[a]

Entry	Catalyst	Yield of TMF (%)
1	LiCl	52
2	$AlCl_3$	33
3	$ZnCl_2$	76
4	$MgCl_2$	54
5	$CaCl_2$	44
6	NaCl	—
7	$FeCl_3$	49
8	$ZnCl_2/SiO_2$	62

[a] Reaction conditions: AcMF (0.501 g, 2.92 mmol), toluene (4 equiv., 11.94 mmol), catalyst (0.250 g, 50 wt%), 120 °C, 3 h.

Fuel properties analysis of various blends

The density of the blend B1, B2, B3, and B5 was slightly higher than that of pure diesel, and it was increased with an increase in the vol% of TMF in the diesel blend. The increased density of diesel-TMF blends is advantageous for improved energy content per unit volume. For pure diesel, the density (at 15 °C) was 0.8315 g/cc, which increased to 0.8319, 0.8347, 0.8349, and 0.837 g/cc for blends B1, B2, B3, and B5, respectively. The kinematic viscosity at 40 °C was higher in the case of diesel and decreased with an increase in the blend percentage from 2.781 cSt to 2.584 cSt. The pour point of the diesel and the diesel blends remains constant at −6 °C, which tells that the diesel and all blends remain pourable or flow at −6 °C. It is an essential parameter for evaluating the cold flow properties of the fuel. The flash point, acid value, and sulfur content were in the acceptable range of diesel fuel. The testing methods, units, and various physiochemical properties of diesel and diesel blends are mentioned in Table 3.

Utilization of TMF–diesel blends as fuel for diesel engines

Performance characteristics. The performance studies evaluate how efficiently a diesel engine converts fuels into useful work under various conditions. Brake Thermal Efficiency (BTE) is defined as the efficiency with which the chemical energy of the fuel is converted into useful mechanical work. The BTE can be calculated by the ratio of brake power output to the fuel energy input. It was observed that the BTE in the diesel blends (B1, B2, B3, and B5) was more in comparison with pure diesel, which signifies that the engine is converting chemical energy into that less heat escapes through the exhaust. Fig. 1 shows BTE at various loads (25%, 50%, 75%, and 100%) of pure diesel and diesel blends (B1, B2, B3, and B5). At lower engine loads (25% and 50%), the BTE increases with an increase in the blend percentage (1–5%), which can be attributed to the presence of oxygenated functional groups of TMF in the blend fuel, which enhances the combustion efficiency due to the improved atomization. However, at higher loads (75%), non-monotonic behaviour was observed. While 1% and 2% blends slightly improve the BTE due to better combustion, the 3% and 5%

Table 3 Physiochemical properties of diesel and the diesel blends with TMF

Physicochemical properties	Testing methods	Unit	Diesel	B1	B2	B3	B5
Density at 15 °C	ASTM D4052-22	g/cc	0.8315	0.8319	0.8347	0.8349	0.837
Kinematic viscosity at 40 °C	ASTM D7042-21a	cSt	2.781	2.718	2.681	2.639	2.584
Pour point	ASTM D5950-14	°C	−6	−6	−6	−6	−6
Flash point	ASTM D93-20	°C	47	37	41	45.5	46.5
Sulfur content	ASTM D7220-22	ppm	6	10.5	10	10	9.5
Calorific value	ASTM D240-19	MJ kg^{-1}	45.502	45.988	45.531	44.824	44.824
Acid value	ASTM D664-24	mg KOH g^{-1}	0.06	0.06	0.06	0.12	0.15

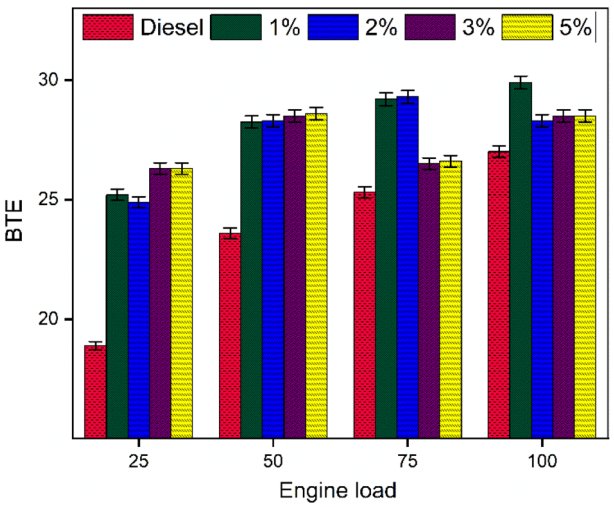

Fig. 1 Variation of BTE with engine loads.

blends show a decrease in BTE. This trend can be attributed to the lower volatility of TMF used as a blend compared to diesel. At higher blend percentages, there may be a delay in the evaporation, which leads to longer ignition delays and combustion phasing mismatches. As the load increased, the amount of fuel injected per cycle increased, increasing the in-cylinder pressure and improving the combustion process. The complete combustion allows a greater proportion of the fuel's chemical energy to be converted into useful mechanical energy, thereby enhancing the BTE. It was observed that BTE for pure diesel and diesel blends increased with an increase in the load, even though some minor deviations were observed.

An uncertainty analysis was carried out to study the accuracy of the instruments while performing the experiments. The uncertainty in BTE was determined based on the propagation of errors from individual measured parameters, following the root-sum-square method. The uncertainty analysis is included in the SI.

Combustion analysis. The combustion analysis inside the engine can be explained by in-cylinder pressure. The maximum in-cylinder pressure (CP-max) refers to the highest pressure reached during a single engine cycle inside the combustion chamber of an internal combustion engine. The average value of 100 engine cycles was calculated at each load for various diesel blends (B1, B2, B3, and B5) to record the CP-max, and these values are depicted in Fig. 2. In general, the CP-max increased with high engine load due to increase in temperature with higher compression and more fuel intake in unit time. Diesel blends exhibit variable ignition characteristics depending on the volatility. While some ignites early due to higher oxygen content, whereas other may ignite later due to slower evaporation. A blend that causes earlier combustion phasing may raise CP-max, while one that burns slowly (due to slow evaporation or late ignition) decreases the CP-max. At 100% engine load (18 kg), the CP-max value was 53.4 bar. The value gradually decreases to 51.29, 51.22, 43.8, and 43.77 bar for B1, B2, B3, and B5, respectively. The trend of CP-max value can be justified by the presence of oxygen atoms in TMF that assist in the combustion of diesel-TMF blends, improving combustion efficiency and reducing emissions. It was observed that the CP-max for pure diesel and diesel blends (B1, B2, B3, and B5) increased with the load. With an increase in the engine load, more fuel is required to fulfil the increased power demand, resulting in more chemical energy being released during the combustion. The increased heat released leads to higher combustion temperatures, elevating the maximum in-cylinder pressure.

Emission analysis. The impact of blended TMF vol% as blend to diesel on emissions was studied using INDUS 5 Gas Analyser model: PEA 205N. Nitrogen oxides (NOx) emission is primarily temperature dependent, and it was observed that with

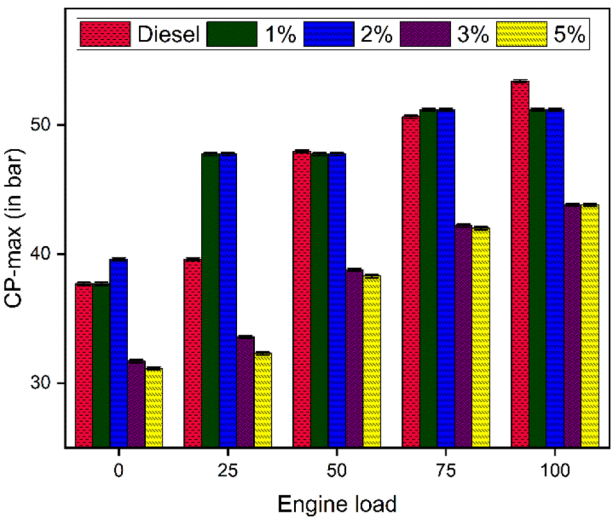

Fig. 2 Variation of CP-max with engine loads.

an increase in the load, the NOx was increased from 8 ppm to 285 ppm for pure diesel. For 1% blend (B1), the NOx increased from 4 ppm to 280 ppm with an increase in the load. At 75% load (13.5 kg), the NOx concentration for diesel was 240 ppm, which decreased to 237, 222, 210, and 206 ppm for B1, B2, B3, and B5, respectively. At 100% engine load (18 kg), the NOx concentration for diesel was 285 ppm, which decreased to 280, 269, 246, and 239 ppm for B1, B2, B3, and B5, respectively. The NOx emission (in ppm) of diesel and diesel blends at various loads are mentioned in Fig. 3. Increasing the TMF blend ratio from B1 to B5 decreased the CP-max, which implies a reduction in maximum combustion temperature, thus suppressing the NOx formation. The NOx emission increased with the increase in the engine load for pure diesel and diesel blends (B1, B2, B3, and B5). As the load increases, the fuel injected per cycle also increases to meet the elevated power demand. Consequently, more heat is released during combustion, resulting in significantly higher in-cylinder pressure and temperature, providing favourable conditions for NOx formation.

Carbon monoxide is generated by the incomplete combustion of fuels (carbon and oxygen) inside the combustion chamber. A consistent reduction in CO emission was observed across all diesel blends compared to diesel. At 75% load (13.5 kg), the CO concentration for diesel was 0.062% & which decreased to 0.058, 0.057, 0.056, and 0.052% for B1, B2, B3, and B5 respectively whereas at 100% load (18 kg), the CO concentration for diesel was 0.251% which decreased to 0.246, 0.221, 0.202, and 0.181% for B1, B2, B3, and B5 respectively. The CO emission (%) of diesel and diesel blends at various loads are mentioned in Fig. 4. The decrease in the percentage of CO can be attributed to the better combustion of diesel blends due to the presence of TMF as a fuel oxygenate. As the engine load increases from 0% to 75%, a gradual increase in the CO emission was observed for pure diesel and diesel blends. At 100% load, a sharp rise in CO emission was recorded. The combustion process becomes more intense and rapid with an increase in the engine load, reducing the residence time available for the complete oxidation of CO to CO_2, which increases the CO emission.

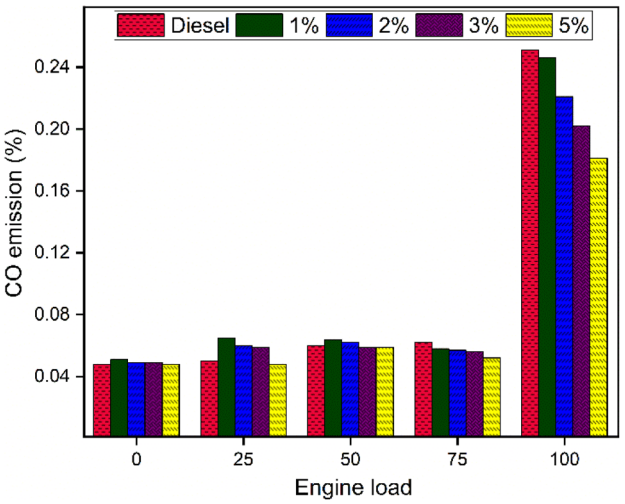

Fig. 4 Emission of carbon monooxide (%) at various engine loads.

The oxidation tendency of carbon atoms in fuel mixtures and an inadequate amount of oxygen within the combustion chamber are indicated by carbon dioxide emissions. Density, viscosity, oxygen content, carbon content, and air-to-fuel ratio affect carbon dioxide emissions. The variation of CO_2 with diesel and various diesel blends at different loads is shown in Fig. 5. It was observed that the diesel has higher CO_2 emission, and it decreased as the blending of TMF increased. No significant decrease in the CO_2 emission was observed with increasing percentage of TMF in the blended fuels indicates that the total carbon conversion to CO_2 remain relatively stable as carbon content of TMF is comparable to diesel, CO_2 levels are not significantly impacted. Higher loads typically lead to more complete combustion due to elevated in-cylinder pressure and temperature, which enhances the oxidation reactions. This

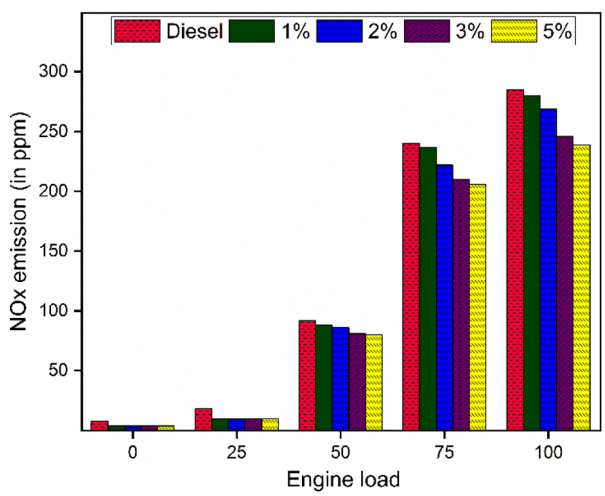

Fig. 3 Emission of NOx (in ppm) at various engine loads.

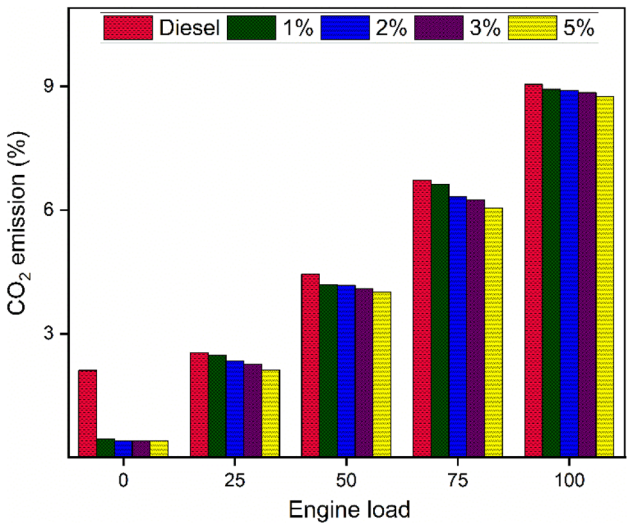

Fig. 5 Emission of carbon dioxide (in %) at various engine loads.

improved combustion reduces the partial combustion product CO, and simultaneously increases the conversion of carbon fuel to CO_2. It is evident that the CO_2 emission increases with an increase in load for pure diesel and diesel blends.

The unburnt hydrocarbons (UHC) are generated due to the partial or incomplete combustion inside the combustion chamber. UHC was lowest in the 5% blend and increased with an increase in the load from 0% to 100% even though some fluctuations were observed. This trend hints at the improved combustion efficiency due to incorporating TMF as a fuel oxygenate that reduces the oxygen demand of the fuel blend during combustion. Typically, UHC decreases with increasing engine load because of better combustion at higher combustion temperature inside the cylinder (higher compression ratio). However, the fuel/air ratio is increased at high engine load to generate more power and avoid overheating the cylinder. Therefore, the trend may deviate and even reverse. Both increasing and decreasing trends of UHC with increasing engine load have been reported in the literature. At higher engine load (75% & 100%), a noticeable decrease in UHC was observed for the 5% TMF-diesel blend compared to unblended diesel. The UHC of diesel and diesel blends at various loads is shown in Fig. 6.

The residual (unreacted) oxygen in emission analysis is an important indicator of combustion efficiency, air-fuel ratio, and oxygen availability. It was observed that the unreacted oxygen in the emission increased from B1 through B5. The above result can be attributed to the increase in the oxygen percentage due to the rise in the vol% of TMF in the diesel. The O_2 emissions decrease with an increase in the load, which can be justified by using more oxygen at a higher load for converting chemical energy into mechanical energy. The O_2 of diesel and diesel blends at various loads is shown in Fig. 7. With an increase in the load, the oxygen emission decreases for pure diesel and diesel blends (B1, B2, B3, and B5). The air-fuel ratio becomes richer at higher loads, resulting in more oxygen utilization during combustion. Therefore, less unreacted oxygen remains in the exhaust gases, resulting in lower oxygen concentration.

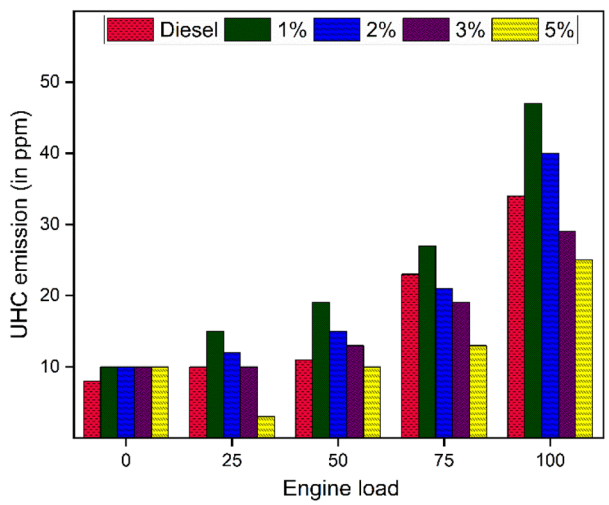

Fig. 6 Emission of unburnt hydrocarbon (in ppm) at various engine loads.

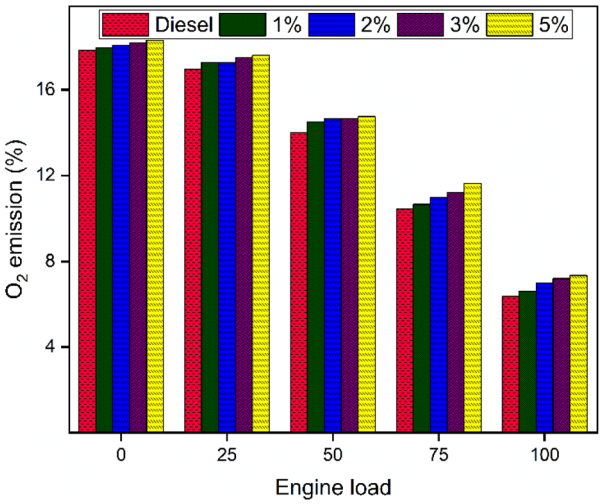

Fig. 7 Emission of O_2 (in %) at various engine loads.

Conclusions

In conclusion, TMF was prepared using the Friedel–Crafts reaction between carbohydrate-derived AcMF and toluene using $ZnCl_2$ as a catalyst and nitromethane as a solvent. Toluene can also be sourced inexpensively from petroleum to produce TMF as a hybrid biofuel. TMF was used as a fuel oxygenate and blended (1–5 vol%) with petrodiesel. Engine performance and emission profiles of the diesel blends were studied in a four-stroke single-cylinder internal combustion engine. The results show that the BTE increases in the diesel blends with a higher percentage of TMF, whereas emission of NOx, CO, CO_2, and UHC decreases. Adding TMF in diesel as a fuel oxygenate improved the fuel properties of the diesel blends and led to better engine performance and cleaner emissions.

Author contributions

Abhishek Kumar Yadav performed the experiments and analyzed the data. Sandeep Kumar Yadav helped in collecting the physicochemical characteristics data of the fuel blends. Kumar G N and Vasudeva Madav assisted in the engine performance and emission analysis and edited the manuscript. Saikat Dutta conceptualized the work, supervised, and wrote the original draft.

Conflicts of interest

There are no conflicts to declare.

List of abbreviations

AcMF	5-(Acetoxymethyl)furfural
ASTM	American Society for Testing and Materials

HMF	5-(Hydroxymethyl)furfural
TLC	Thin-layer chromatography
TMF	5-(Tolylmethyl)furfural

Data availability

The data supporting this article have been included as part of the SI.

ESI contains the IC engine images, reaction setup and purification process images, visual pictures diesel and diesel-blend, and NMR of TMF. See DOI: **https://doi.org/10.1039/d5ra04020e**.

Acknowledgements

The author thanks the central library of NITK, Surathkal, for providing access to academic journals and databases. The authors thank the Engine Testing Facility at NITK, Surathkal. This research received funding from the Science and Engineering Research Board (SERB) under the Core Research Grant (CRG) scheme (File no. CRG/2022/009346).

References

1 C. R. Knittel, *J. Econ. Perspect.*, 2012, **26**, 93–118.
2 U. K. Bhui, in *Macromolecular Characterization of Hydrocarbons for Sustainable Future*, ed. U. K. Bhui, Springer Singapore, Singapore, 2021, pp. 3–18.
3 I. Heim, A. C. Vigneau and Y. Kalyuzhnova, *Reg. Stud.*, 2023, **57**, 181–195.
4 R. Kumar, V. Strezov, H. Weldekidan, J. He, S. Singh, T. Kan and B. Dastjerdi, *Renewable Sustainable Energy Rev.*, 2020, **123**, 109763.
5 A. I. Osman, N. Mehta, A. M. Elgarahy, A. Al-Hinai, A. H. Al-Muhtaseb and D. W. Rooney, *Environ. Chem. Lett.*, 2021, **19**, 4075–4118.
6 G. Dhamodaran, G. S. Esakkimuthu, T. Palani and A. Sundaraganesan, *Emergent Mater.*, 2023, **6**, 1393–1413.
7 P. Karin, A. Tripatara, P. Wai, B.-S. Oh, C. Charoenphonphanich, N. Chollacoop and H. Kosaka, *Case Stud. Chem. Environ. Eng.*, 2022, **6**, 100249.
8 A. T. Hoang, S. Nižetić and A. I. Ölçer, *Fuel*, 2021, **285**, 119140.
9 A. Mittal, H. M. Pilath and D. K. Johnson, *Energy Fuels*, 2020, **34**, 3284–3293.
10 F. Menegazzo, E. Ghedini and M. Signoretto, *Molecules*, 2018, **23**, 2201.
11 Y. Shao, Y. Ding, J. Dai, Y. Long and Z.-T. Hu, *Green Synth. Catal.*, 2021, **2**, 187–197.
12 N. Vinod and S. Dutta, *Sustainable Chem.*, 2021, **2**, 521–549.
13 S. H. Shinde and C. V. Rode, *ACS Omega*, 2018, **3**, 5491–5501.
14 D. S. Ryabukhin, D. N. Zakusilo, M. O. Kompanets, A. A. Tarakanov, I. A. Boyarskaya, T. O. Artamonova, M. A. Khohodorkovskiy, I. O. Opeida and A. V. Vasilyev, *Beilstein J. Org. Chem.*, 2016, **12**, 2125–2135.
15 K. S. Arias, M. J. Climent, A. Corma and S. Iborra, *Energy Environ. Sci.*, 2015, **8**, 317–331.
16 C. Rosenfeld, J. Konnerth, W. Sailer-Kronlachner, P. Solt, T. Rosenau and H. W. G. van Herwijnen, *ChemSusChem*, 2020, **13**, 3544–3564.
17 H. N. Anchan and S. Dutta, *Biomass Convers. Biorefin.*, 2023, **13**, 2571–2593.
18 J. Bueno Morón, F. Arbore, G. P. M. van Klink, M. Mascal and G. M. Gruter, *ChemSusChem*, 2024, **17**, e202400495.
19 H. Arunkumar, S. H. Manjunath and N. V. K. Reddy, *Int. J. Vehicle Structures and Systems*, 2021, **13**, 10.
20 A. K. Yadav, N. S. Bhat, S. Kaushik, A. H. Seikh and S. Dutta, *RSC Adv.*, 2024, **14**, 3096–3103.
21 C. Forsberg, *Appl. Energy*, 2023, **341**, 121104.
22 N. S. Bhat, A. K. Yadav, M. Karmakar, A. Thakur, S. S. Mal and S. Dutta, *ACS Omega*, 2023, **8**, 8119–8124.
23 S. Shinde, K. Deval, R. Chikate and C. Rode, *ChemistrySelect*, 2018, **3**, 8770–8778.
24 N. S. Bhat, S. L. Hegde, S. Dutta and P. Sudarsanam, *ACS Sustainable Chem. Eng.*, 2022, **10**, 5803–5809.
25 S. Dutta, *Energy Fuels*, 2023, **37**, 2648–2666.
26 N. Yilmaz and A. Atmanli, *Fuel*, 2017, **210**, 75–82.
27 A. Ibrahim, *Eng. Sci. Technol. Int. J.*, 2018, **21**, 1024–1033.
28 M. R. Atelge, *Fuel*, 2022, **325**, 124903.